Available online at www.sciencedirect.com
ScienceDirect
Journal of Sound and Vibration 318 (2008) 193–205
JOURNAL OF SOUND AND VIBRATION
www.elsevier.com/locate/jsvi

Vibration reduction by using the idea of phononic crystals in a pipe-conveying fluid

Dianlong Yu*, Jihong Wen, Honggang Zhao, Yaozong Liu, Xisen Wen

Institute of Mechatronical Engineering, and The PBG Research Center, National University of Defense Technology, Changsha 410073, China

Received 15 October 2007; received in revised form 3 April 2008; accepted 7 April 2008
Handling Editor: J. Lam
Available online 6 June 2008

Abstract

Flexural vibration in a pipe system conveying fluid is studied. The pipe is designed using the idea of the phononic crystals. Using the transfer matrix method, the complex band structure of the flexural wave is calculated to investigate the gap frequency range and the vibration reduction in band gap. Gaps with Bragg scattering mechanism and locally resonant mechanism can exist in a piping system with fluid loading. The effects of various parameters on the gaps are considered. The existence of flexural vibration gaps in a periodic pipe with fluid loading lends new insight into the vibration control of pipe system.

1. Introduction

Elastic wave propagation in periodic structures has been researched for years [1–3]. The vibration response of periodic structures has been applied primarily to pass band and stop band analysis. But most of this work dealt with one-dimensional (1D) structures.

In the last decade, the propagation of elastic or acoustic waves in periodic composite materials called phononic crystals (PCs) has received considerable attention [4–13]. The emphasis of these studies was laid on the existence of complete elastic band gaps within which both sound and vibration are forbidden. This is of interest for applications such as frequency filters, vibrationless environments for high-precision mechanical systems, and transducer design.

There are two kinds of gap formation mechanism for PCs, Bragg scattering mechanism [4–6] and locally resonant (LR) mechanism [7–9].

The studies have shown that the existence of the Bragg gaps is strongly connected with a large acoustic impedance ratio between the scatterers' and the matrix' material [9]. The center frequencies are always given by Bragg's condition $f = n(v/2a)$ $(n = 1, 2, 3, \ldots)$, where v is the elastic velocity of the matrix material and a is the lattice constant [9]. For PCs with gaps induced by the Bragg scattering mechanism, the spatial modulation of the elasticity must be of the same order as the wavelength in the gap. Thus, it is not practical for shielding

*Corresponding author. Tel./fax: +86 731 4574975.
E-mail address: dianlongyu@nudt.edu.cn (D. Yu).

0022-460X/$ - see front matter © 2008 Elsevier Ltd. All rights reserved.
doi:10.1016/j.jsv.2008.04.009

acoustic sound, because the structure would have to be the size of outdoor sculptures in order to shield environmental noises [7].

The pioneering work of Liu et al. [7] has opened additional field of PCs. The authors studied three-dimensional (3D) PCs consisting of cubic arrays of coated lead spheres (the coating is a thin film of a soft material) immersed in an epoxy matrix, i.e., LR PCs. The frequency of a LR gap is dictated by the frequency of the resonance, and is independent of orderness, periodicity, and symmetry unless there is a high concentration of resonating units so that they couple strongly with each other [10]. The LR gaps can exist in a frequency range of two orders of magnitude lower than the one resulting from the Bragg scattering.

The conventional gaps in the periodic structures can be attributed to the Bragg mechanism using PCs theory. Similarly we can introduce the LR gaps into the periodic structures. Also by using the PCs calculation method, the vibration propagation property of two-dimensional (2D) and 3D periodic structures can be dealt with conveniently. Vibration band gaps in PCs have been found experimentally and theoretically [11–13].

Vibration analysis of piping systems conveying fluid has received considerable attention due to its wide application to areas such as the designing of heat exchanger tubes, main steam pipes, and hot/cold leg pipes in nuclear steam supply systems, oil pipelines, pump discharge lines, marine risers, and others [14]. Vibration analysis of pipe systems is something that has been studied early on [14–17].

There are many vibration modes existing in pipe system that convey fluid, such as longitudinal vibration, torsional vibration, flexural vibration, and their coupled vibrational modes. As a typical and important vibration mode, flexural vibration was studied early on. In Ref. [15], the free flexural wave propagation in the periodically supported, infinite piping system conveying fluid was studied. They designed a pipe with periodic supports to reduce the vibration. Flexural vibration gaps formed with the Bragg scattering mechanism can exist in the pipe with periodic supports. To our knowledge, no work appears in the open literature studying Bragg band gaps in periodic pipe walls or LR gaps in the pipe.

In this paper, we investigate the flexural vibration band gaps in the periodic pipe system conveying fluid. Both the Bragg scattering mechanism and the LR mechanism are introduced into the pipe system conveying fluid. The band structure for infinite periodic cells is calculated by the transfer matrix (TM) method. The results show that vibration band gaps can control vibration propagation through the pipe system conveying fluid. Using the idea of PCs, the existing band gaps will provide a new way to reduce the vibration of pipe-conveying fluid.

2. Models and transfer matrix method

2.1. Equations of motion

For the Euler-type pipe conveying fluid at a constant velocity v, if gravitational forces, internal damping, externally imposed tension, and pressurization effects are neglected, the well-known governing equation of flexural vibration becomes [16,17]

$$EI\frac{\partial^4 w}{\partial x^4} + m_f v^2 \frac{\partial^2 w}{\partial x^2} + 2m_f v \frac{\partial^2 w}{\partial x \partial t} + (m_f + m_p)\frac{\partial^2 w}{\partial t^2} = 0, \tag{1}$$

where w is the flexural displacement, E is Young's modulus of the pipe wall material, I is the area moment of inertia with respect to the axis perpendicular to the pipe axis, EI is the flexural rigidity of the pipe, m_f and m_p are fluid and pipe masses per unit length, respectively, and v and t are the constant uniform fluid velocity and time, respectively.

For a harmonic traveling wave $w(x,t) = W\,\mathrm{e}^{\mathrm{i}(\omega t - kx)}$, one can find the dispersion relation of Eq. (1):

$$EIk^4 - m_f v^2 k^2 + 2m_f v\omega k - (m_f + m_p)\omega^2 = 0. \tag{2}$$

For a given ω, the wavenumber roots of Eq. (2) include two different real roots and a conjugate pair of complex roots, designated [16] $k_d, -k_u, k_R \pm \mathrm{i}k_I$. The positive and negative real wavenumbers describe the propagating waves in positive and negative directions. And the conjugate root pair describes the near-field waves (non-propagating, spatially decaying). Also, the wavenumbers depend on the frequency ω and flow speed v [17].

The harmonic solution of Eq. (1) is

$$w(x,t) = e^{i\omega t}(W_1 e^{-ik_1 x} + W_2 e^{-ik_2 x} + W_3 e^{-ik_3 x} + W_4 e^{-ik_4 x}), \tag{3}$$

where the wavenumber k_i ($i = 1, 2, 3, 4$) is given by $k_1 = k_d$, $k_2 = -k_u$, $k_3 = k_R + ik_I$, $k_4 = k_R - ik_I$.

For the Euler pipe without fluid loading, the pipe can be treated as Euler beam. The equation of motion is given as

$$EI\frac{\partial^4 w}{\partial x^4} + m_p\frac{\partial^2 w}{\partial t^2} = 0. \tag{4}$$

And the harmonic solution of Eq. (2) for the pipe without fluid loading is

$$w(x,t) = e^{i\omega t}(a^+ e^{-ikx} + a_N^+ e^{-kx} + a^- e^{ikx} + a_N^- e^{ikx}), \tag{5}$$

where the subscript N denotes the near-field wave component. The wavenumber k is given by

$$k = \sqrt[4]{m_p\omega^2/EI}. \tag{6}$$

2.2. Model and TM for Bragg mechanism

Fig. 1 shows a periodic binary composite pipe system. The system consists of an infinite repetition of alternating pipe A with length a_1 and pipe B with length a_2. Thus, the PCs pipe's lattice constant is $a = a_1 + a_2$. Pipe A and pipe B are made up of different materials, A and B, respectively.

For pipe with fluid loading, the continuities of displacement, slope, bending moment and shear force at the interfaces between cell $n-1$ and n, i.e. $x = na$ give:

$$w_{n,A}(0) = w_{n-1,B}(a), \tag{7a}$$

$$w'_{n,A}(0) = w'_{n-1,B}(a), \tag{7b}$$

$$E_A I_A w''_{n,A}(0) = E_B I_B w''_{n-1,B}(a), \tag{7c}$$

$$E_A I_A w'''_{n,A}(0) = E_B I_B w'''_{n-1,B}(a). \tag{7d}$$

One can obtain the matrix form of Eqs. (7)

$$\mathbf{K}\mathbf{W}_{n,A} = \mathbf{H}\mathbf{W}_{n-1,B}, \tag{8}$$

where $\mathbf{W} = [W_1, W_2, W_3, W_4]^T$.

The continuities at the interfaces between pipes A and B in cell n, i.e. $x = na + a_1$, give:

$$w_{n,A}(a_1) = w_{n,B}(a_1), \tag{9a}$$

$$w'_{n,A}(a_1) = w'_{n,B}(a_1), \tag{9b}$$

$$E_A I_A w''_{n,A}(a_1) = E_B I_B w''_{n,B}(a_1), \tag{9c}$$

$$E_A I_A w'''_{n,A}(a_1) = E_B I_B w'''_{n,B}(a_1). \tag{9d}$$

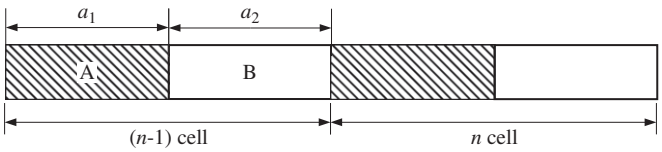

Fig. 1. The sketch map of periodic binary pipe.

The matrix form of Eq. (9) can be written as

$$\mathbf{K}_1\mathbf{W}_{n,A} = \mathbf{H}_1\mathbf{W}_{n,B}. \tag{10}$$

Based on Eqs. (8) and (10), the relation between the nth cell and $(n-1)$th cell is given

$$\mathbf{W}_{n,B} = \mathbf{T}\mathbf{W}_{n-1,B}, \tag{11}$$

where $\mathbf{T} = \mathbf{H}_1^{-1}\mathbf{K}_1\mathbf{K}^{-1}\mathbf{H}$ is the TM.

Due to the periodicity of the infinite structure in the x direction, the vector $\mathbf{W}_n$ must satisfy the Bloch theorem [18]

$$\mathbf{W}_n = \mathrm{e}^{\mathrm{i}qa}\mathbf{W}_{n-1}, \tag{12}$$

where q is the wave vector in the x direction. For convenience, we write all the one-dimension vectors as scalar form in this paper.

It follows that the eigenvalues of the infinite periodic pipe structures with fluid loading are the roots of the determinant

$$\left|\mathbf{T} - \mathrm{e}^{\mathrm{i}qa}\mathbf{I}\right| = 0, \tag{13}$$

where $\mathbf{I}$ is the 4×4 unit matrix. For given ω, Eq. (13) gives the values of q. Depending on whether q is real or has an imaginary part, the corresponding wave propagates through the beam (pass band) or is damped (band gap).

Similarly, one can get the eigenvalues of the infinite periodic pipe structures without fluid loading basing on Eq. (4).

2.3. Model and TM for LR mechanism

Fig. 2 shows a simple model of a pipe with periodical LR structures. The pipe is attached periodically with harmonic oscillators. The LR oscillator consists of the spring k and mass m. The lattice constant is a.

As for the nth LR oscillator, considering the equilibrium condition for all the forces in the y-axis, including the inertial force, one obtains [19,20]

$$f_n(t) - m\frac{\partial^2 Z_n(t)}{\partial t^2} = 0, \tag{14}$$

where $f_n(t)$ is the interactive forces between the LR oscillator and the pipe at the attaching point x_n. $Z_n(t) = V_n \exp(\mathrm{i}\omega t)$ is the displacement of the nth LR oscillator at the center of gravity. The absolute value of V_n is the amplitude of the vibration of the nth LR oscillator.

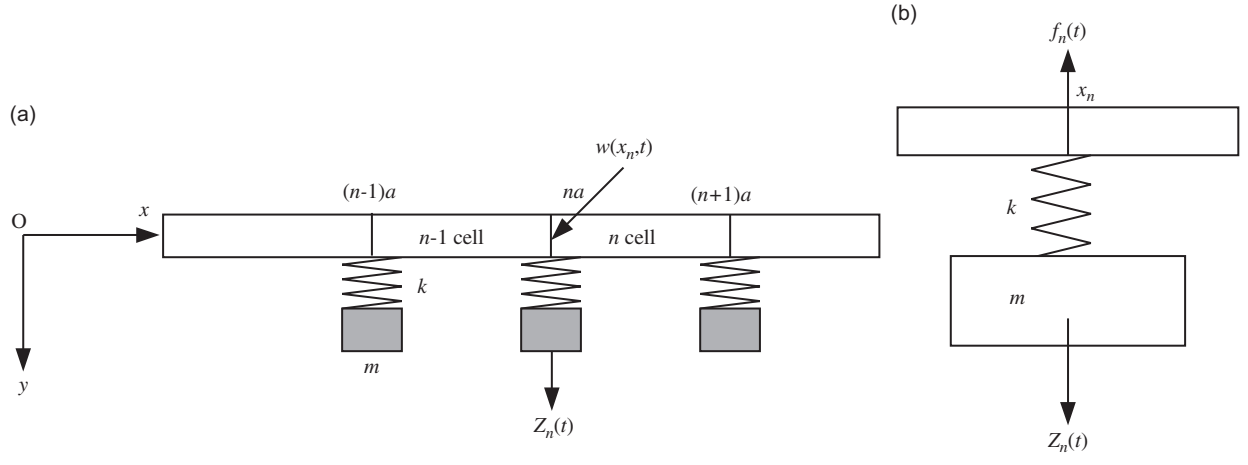

Fig. 2. (a) The sample model of the pipe with LR structures and (b) the fore equilibrium of the nth LR structure.

The force $f_n(t)$ is given by

$$\begin{aligned} f_n(t) &= k[w(x_n,t) - Z_n(t)] \\ &= k[w_n(0) - V_n]\exp(\mathrm{i}\omega t) \\ &\triangleq F_n \exp(\mathrm{i}\omega t), \end{aligned} \tag{15}$$

Substituting Eqs. (15) into Eq. (14) leads to

$$V_n = \frac{k}{k - m\omega^2} w_n(0). \tag{16}$$

These results are now used to address the dispersive relation of the pipe with LR structures. As mentioned in last section, there are two interfaces in one cell for the Bragg system. For the LR structures, however, there is only one interface for the one wall materials in one cell, i.e. the attachment point $x_n = na$. The continuities of displacement, slope, bending moment, and shear force at this interface give:

$$w_n(0) = w_{n-1}(a), \tag{17a}$$

$$w_n'(0) = w_{n-1}'(a), \tag{17b}$$

$$EIw_n''(0) = EIw_{n-1}''(a), \tag{17c}$$

$$EIw_n'''(0) - F_n = EIw_{n-1}'''(a). \tag{17d}$$

Substituting Eqs. (3) and (16) into Eq. (17), one can obtain the transfer relation between cell $n-1$ and cell n,

$$\mathbf{W}_n = \hat{\mathbf{T}}\,\mathbf{W}_{n-1}. \tag{18}$$

Similar to Eq. (12) in Bragg case, the standard eigenvalue problem for the pipe with LR structures can be given as follows:

$$|\hat{\mathbf{T}} - \mathrm{e}^{\mathrm{i}qa}\mathbf{I}| = 0. \tag{19}$$

3. Results and discussion

3.1. Bragg gap properties

The periodic pipe with different wall material parameters is illustrated in Fig. 1(a). As an example, we calculated the band structure with epoxy as material A and aluminum as material B. The fluid in the pipe is water. The elastic parameters employed in the calculations were $\rho_A = 1180\,\mathrm{kg/m^3}$, $E_A = 4.35 \times 10^9\,\mathrm{Pa}$ for epoxy, $\rho_B = 2730\,\mathrm{kg/m^3}$, $E_B = 7.756 \times 10^{10}\,\mathrm{Pa}$ for aluminum, and $\rho_w = 1000\,\mathrm{kg/m^3}$ for water. The inner and outer radii of the pipe are chosen as $r_i = 0.09\,\mathrm{m}$ and $r_o = 0.1\,\mathrm{m}$.

For PCs with gaps induced by the Bragg scattering mechanism, the spatial modulation of the elasticity must be of the same order as the wavelength in the gap. So we must choose large lattice constant to get a low-frequency gap. Here, the lattice constant is chosen to be $a = 2\,\mathrm{m}$, and $a_1 = a_2 = 1\,\mathrm{m}$. The flow speed is $v = 50\,\mathrm{m/s}$.

Fig. 3 illustrates the complex band structure calculated with Eq. (13) for the Bragg system. The real wave vector is illustrated in Fig. 3(a), and the absolute value of the imaginary part of the complex wave vector is illustrated in Fig. 3(b). The shadowed region in Fig. 3(a) indicates the complete band gap between 27–45, 123–201, and 335–411 Hz. As for the two different real wavenumbers, k_1 and k_2, there are two branches for a given frequency ω as shown in Fig. 3(a).

Within the gap ranges, wave vectors k_1 and k_2 have the imaginary components [21]. They are illustrated as continuous lines in Fig. 3(b), which can be used to describe the attenuation properties in the band gaps. From Fig. 3(b), one can see that there is an imaginary wave vector (dashed line) within the frequency range of the pass band. This is due to the near-field wave component k_3 and k_4. The values of k_3 and k_4 have imaginary

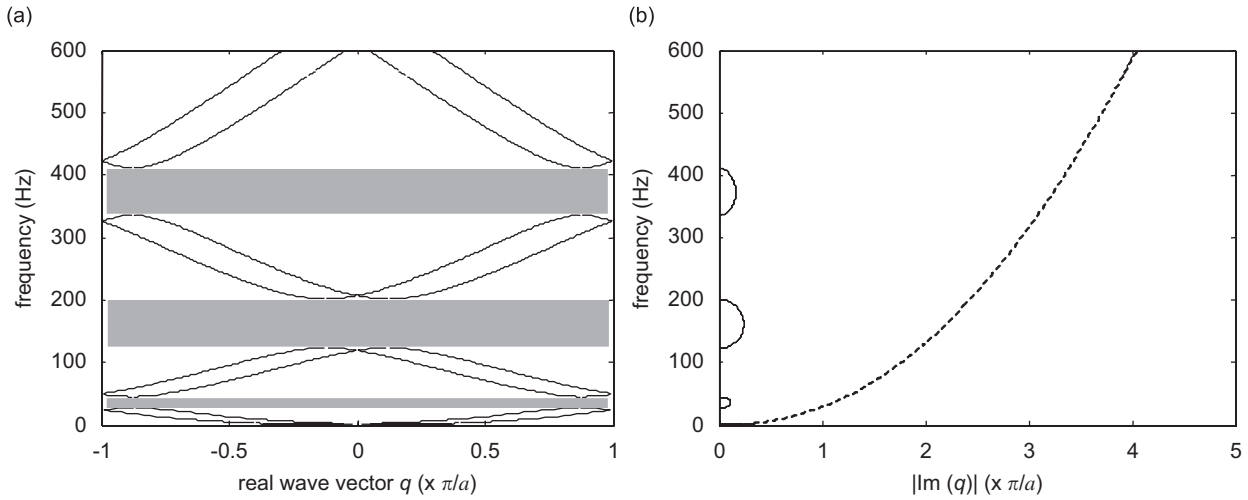

Fig. 3. The complex band structure of the periodic material pipe with fluid loading. The material of pipe A, pipe B and fluid are epoxy, aluminum and water, respectively. The lattice constant $a = 2$ m, internal fluid velocity $v = 50$ m/s: (a) real wave vector and (b) the absolute value of the imaginary part of the complex wave vector. The continuous lines describes the wave vectors k_1, k_2 and dashed line describe the wave vectors k_3 and k_4, respectively.

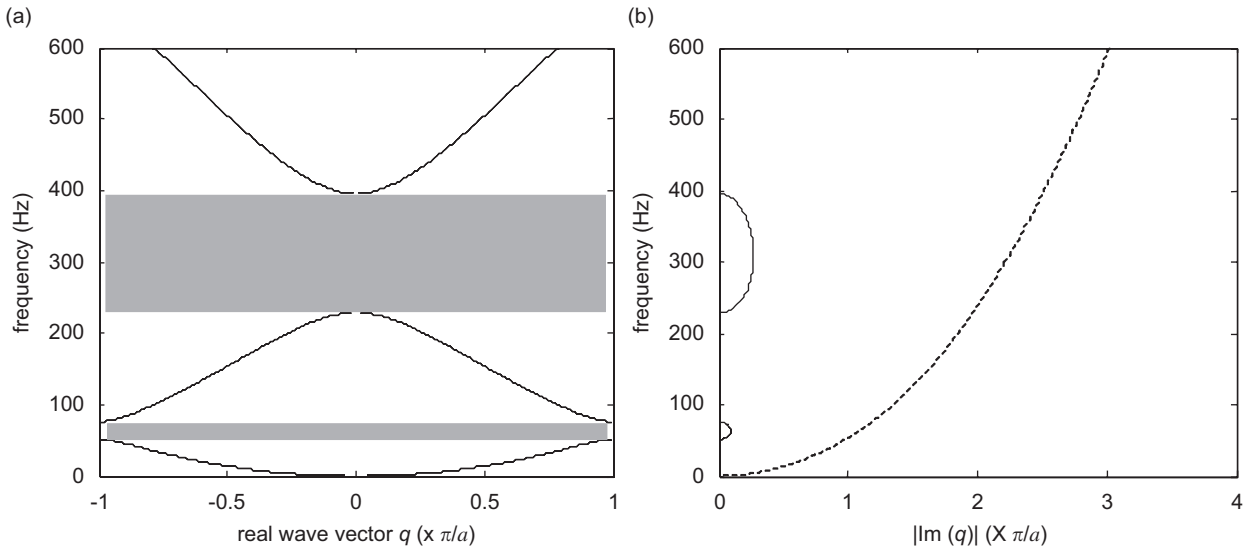

Fig. 4. The complex band structure of the periodic material pipe without fluid loading. The lattice constant $a = 2$ m: (a) real wave vector and (b) the absolute value of the imaginary part of complex wave vector. The continuous lines describe the wave vectors k_1, k_2 and dashed line describe the wave vectors k_3 and k_4, respectively.

parts for all frequencies. And the imaginary part of the complex band structure in Bragg system is symmetric about the center frequency of the gap.

For comparison, we also calculate the complex band structure of the pipe without fluid loading as illustrated in Fig. 4. The material and geometric parameters remain the same as those in Fig. 3. The first two gap ranges are 50–76 and 228–395 Hz. Comparing Fig. 3 with Fig. 4, one finds that the effect of fluid loading is to make the gap frequency lower.

For different internal fluid velocities v, the wavenumbers will change [17]. Thus, we should consider the effect of the internal fluid velocity v on the band gaps. In Fig. 5, the band structure of the pipe with fluid

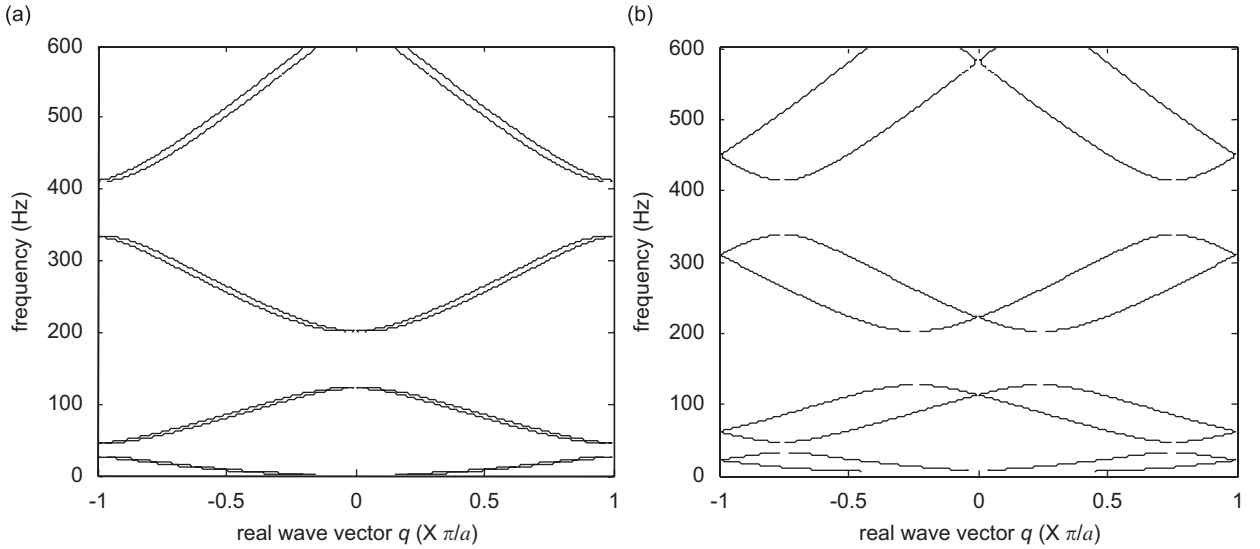

Fig. 5. The band structure of with different internal fluid velocity: (a) $v = 10\,\mathrm{m/s}$ and (b) $v = 100\,\mathrm{m/s}$.

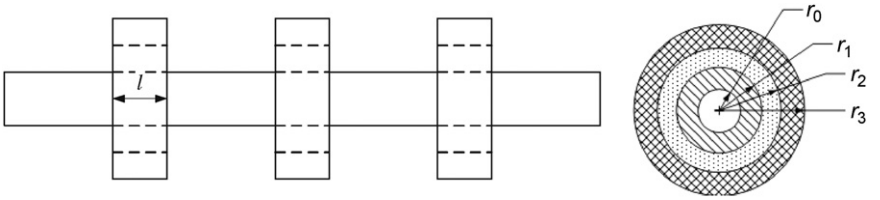

Fig. 6. The sketch of the piping system with LR structure.

loading for velocity $v = 10$ and $100\,\mathrm{m/s}$ is shown. For $v = 10\,\mathrm{m/s}$, the first three gap ranges are 25–44, 122–201 and 334–411 Hz, and for $v = 100\,\mathrm{m/s}$, the gap ranges are 33–47, 127–202 and 338–415 Hz. We find that the gap frequencies become higher in some sort with faster velocity v. The shape of band structure, however, changes visibly due to the difference between real wavenumber k_1, k_2 change greater with a faster velocity v.

3.2. LR gap properties

A pipe with periodic LR structures is shown in Fig. 6. The pipe is constructed from aluminum, whose material parameters are the same as those in Section 3.1. The inner and outer radii of the pipe are chosen as $r_0 = 0.09\,\mathrm{m}$, $r_1 = 0.1\,\mathrm{m}$, respectively. The LR structure is composed of a soft rubber ring and a copper ring. Their outer radii are $r_2 = 0.15\,\mathrm{m}$ and $r_3 = 0.195\,\mathrm{m}$, respectively. The length of the two rings is $l = 2 \times 10^{-2}\,\mathrm{m}$. The area moment of inertia $I = 2.7 \times 10^{-5}\,\mathrm{m}^4$.

For the LR mechanism, we can obtain the low-frequency gap with a smaller lattice constant. Here the lattice constant is chosen as $a = 7.5 \times 10^{-2}\,\mathrm{m}$.

For the rubber ring, the radial stiffness can be calculated as follow [20]:

$$k = \frac{\pi(5 + 3.29H^2)G_{\mathrm{rubber}}l}{\ln(r_2/r_1)} \tag{20}$$

where $H = l/((r_1 + r_2)\ln(r_1/r_2))$ is shape coefficient.

In the calculation, the material parameters are chosen as $\rho_{\mathrm{rubber}} = 1300\,\mathrm{kg\,m^{-3}}$, $G_{\mathrm{rubber}} = 4 \times 10^6\,\mathrm{Pa}$, $\rho_{\mathrm{Cu}} = 8950\,\mathrm{kg\,m^{-3}}$. And the spring stiffness of the rubber ring can be calculated as $k = 3.18 \times 10^6\,\mathrm{N/m}$ basing on Eq. (20).

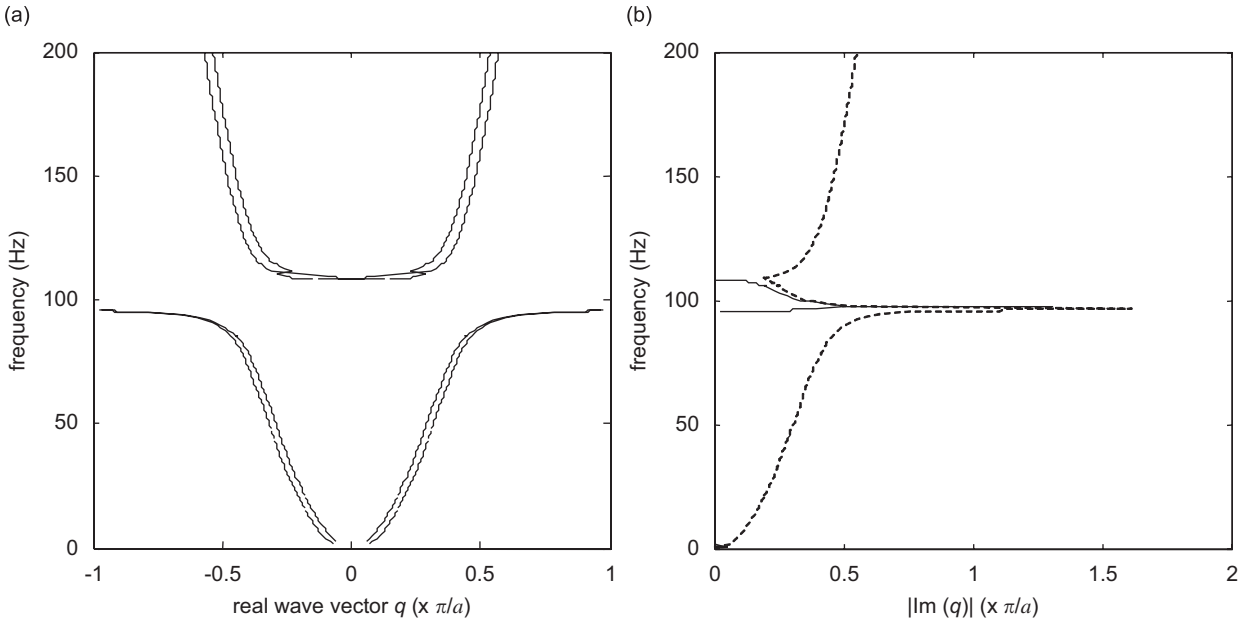

Fig. 7. Complex band structure of the pipe-conveying fluid with infinite LR structures, the lattice constant $a = 7.5 \times 10^{-2}$ m: (a) real wave vector and (b) the absolute value of the imaginary part of complex wave vector. The continuous lines describe the wave vectors k_1, k_2 and dashed line describe the wave vectors k_3 and k_4, respectively.

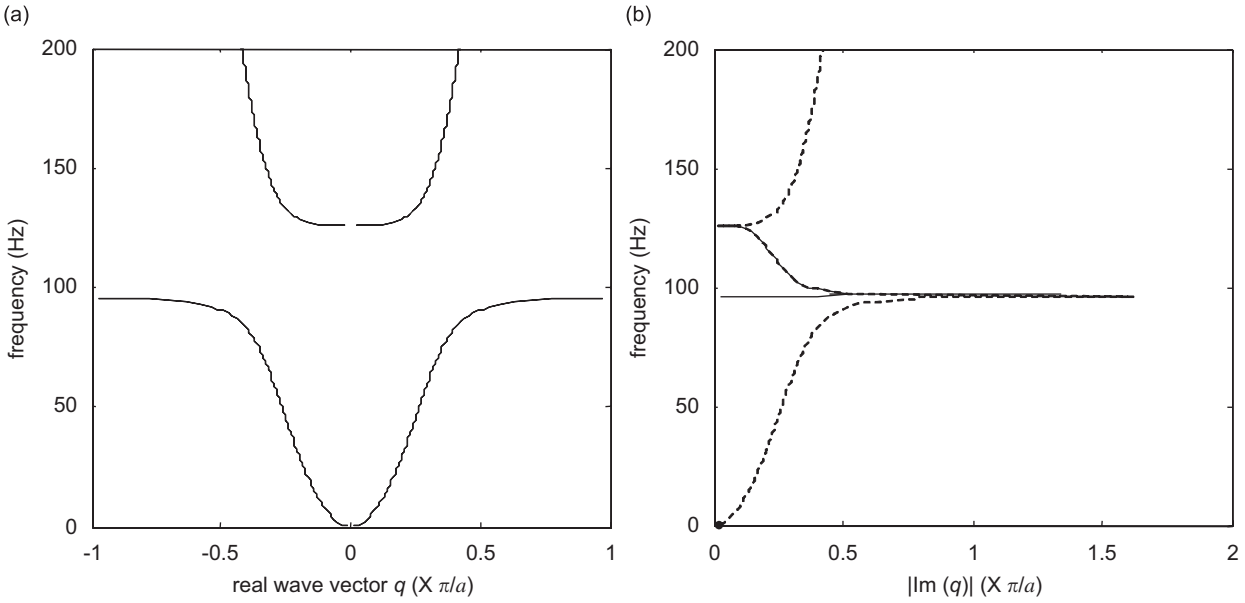

Fig. 8. Complex band structure of the pipe without fluid loading with infinite LR structures, the lattice constant $a = 7.5 \times 10^{-2}$ m: (a) real wave vector and (b) the absolute value of the imaginary part of complex wave vector. The continuous lines describe the wave vectors k_1, k_2 and dashed line describe the wave vectors k_3 and k_4, respectively.

Fig. 7 illustrates the complex band structure calculated with Eq. (19) for the pipe with LR structures. We observe one complete band gap extending from a frequency of 95 Hz up to 108 Hz. One can see that the curve shown in Fig. 7(b) has an asymmetric peak. The attenuation is the strongest at the low-frequency end of the gap and it become weaker with increasing frequency. This is a typical characteristic of the Fano-like interference phenomena in PCs with LR structures [8].

The LR gap in the pipe without fluid loading is illustrated in Fig. 8. The gap range is 95–125 Hz. Comparing Fig. 7 with Fig. 8, one can see that the start frequencies of the LR gap are the same. This is because the start frequency of the LR gap is due to the resonant of the oscillator at $1/2\pi\sqrt{k/m}$. For the pipe without fluid loading, the total mass in one cell including the pipe wall and fluid become smaller. The upper edge of the LR gap is inversely related to the base structure mass [22]. As such, the upper edge of the LR gap in Fig. 8 is higher than that in Fig. 7.

3.3. Bragg gap couple with LR

As we all know, Bragg gaps are dependent on the lattice constant and the LR gaps are dependent on the resonant frequency of the LR oscillator. If we only change the lattice constant, the beginning frequency of the Bragg gap will change, but the LR gap will not be influenced.

While vibration propagates through a pipe with LR structure, the attaching point will reflect the elastic wave. This reflection satisfies the Bragg mechanism, so the Bragg gap can exist in the pipe with LR structure. For a small lattice constant, the Bragg gap frequency is higher than that of LR and it separates from the LR gap. Bragg gaps in PCs with LR structures were not studied. However, for the pipe system, the length is enough for bigger lattice. We can change only the lattice constant to consider the effect of the reflection on the LR gap. Other parameters are the same as those in Fig. 7. Fig. 9 illustrates the band structure calculated with Eq. (13) for the pipe-conveying fluid with LR structures. The lattice constant is $a = 1$ m. We can find two gaps in the range of 0–600 Hz. The first one is the LR gap with a frequency range of 95–125 Hz. The second of these is the Bragg gap whose frequency range is 352–359 Hz. In this case, the Bragg gap separates from the LR gap and it will not affect the LR gap.

If the lattice constant is chosen as 3 m, the Bragg gap frequency will become lower than the LR gap as shown in Fig. 10. In this case, the first gap is a Bragg gap with frequency range of 36.5–39.5 Hz and the second gap is a LR gap with range of 95–103 Hz.

For the bigger lattice constant, the base structure mass in one cell including the pipe wall and fluid become larger. Thus, the upper edge of the LR gap in Fig. 10 is lower than that in Fig. 9.

At the resonant frequency of the oscillator, the harmonic forces from the oscillators to the pipe split the original Bragg dispersion curves, and the LR gap is generated. For different lattice constants, the original Bragg dispersion curves will change, so the aspect of the LR gaps in Figs. 9 and 10 are different.

Fig. 11 illustrates the band gap for a lattice constant of 1.9 m. The band gap frequency range is from 77 to 122 Hz. The resonant frequency exists in the gap. Compared to the data in Fig. 9, this gap range is wider.

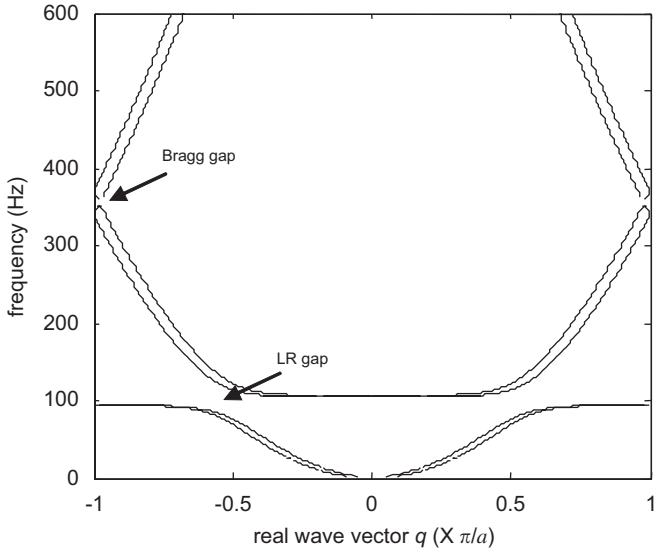

Fig. 9. Band structure of the pipe with fluid loading with infinite LR structures, the lattice constant $a = 1$ m.

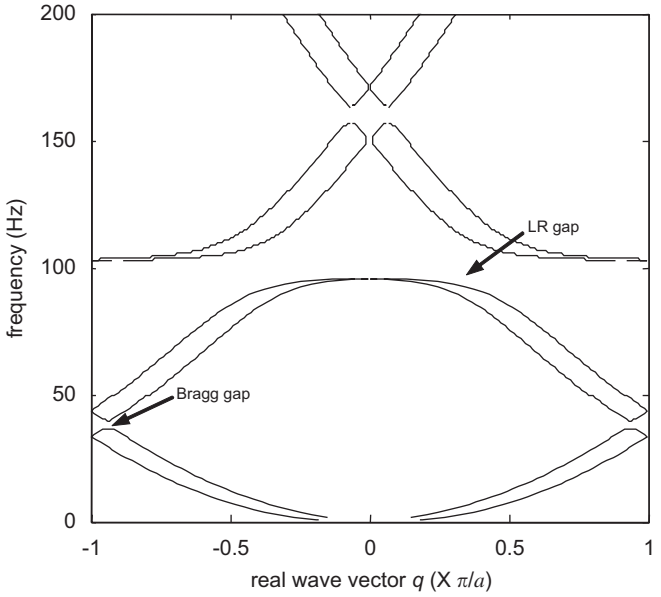

Fig. 10. Band structure of the pipe with fluid loading with infinite LR structures, the lattice constant $a = 3$ m.

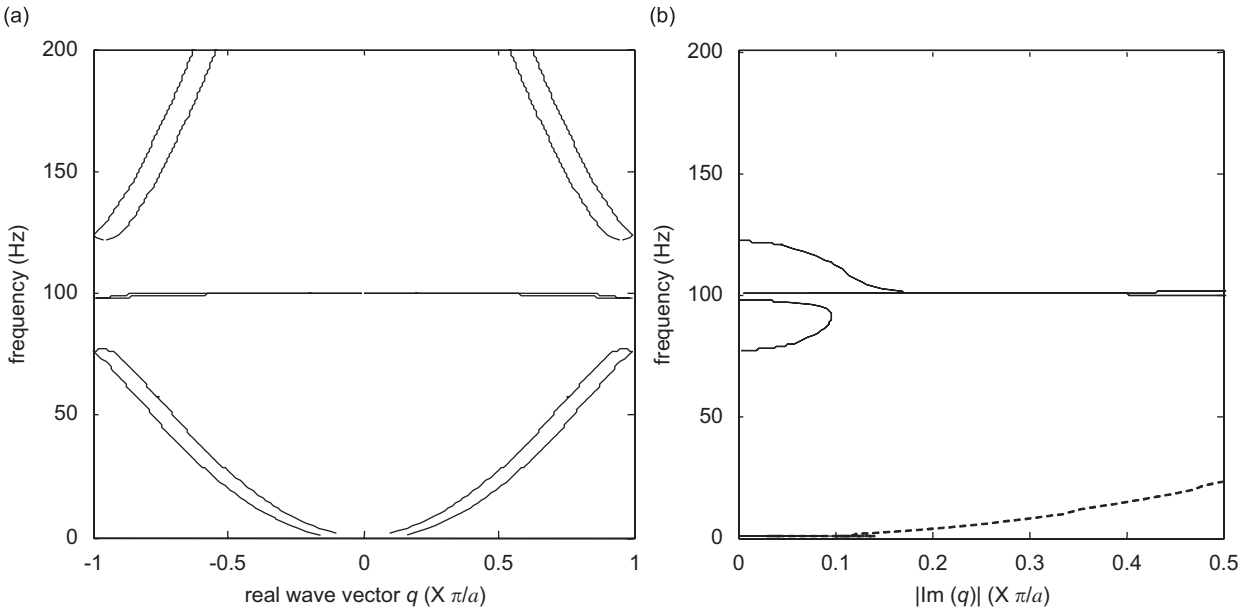

Fig. 11. Complex band structure of the pipe with fluid loading with infinite LR structures, the lattice constant $a = 1.9$ m.

This is due to the LR gap connecting with the Bragg gap as illustrated in the Fig. 11(b). We find the band corresponding to the resonant of oscillator in the gap is very flat. Therefore, the group velocity $\partial\omega/\partial k$ is close to zero. The vibration at this resonant frequency will be localized and the vibration propagation will be very slow. This shows that the resonant effect corresponding to this flat band is very strong. For a bigger or smaller lattice, the effect of the resonance will become weaker because the band is not so flat. This also shows that the coupling between the Bragg scattering mechanism and the LR mechanism is benefited by widening the gap. Also, the larger lattice constant is helpful in decreasing the additional mass for a pipe system.

3.4. Periodic supports by LR

In the design of a piping system, the pipe supports have very important design features from the standpoint of resisting system loads [15]. It has been shown that if the dominant frequency contents in the excitation loads are known, a proper design of periodic supports for reducing the vibration in those frequency bands is possible.

Here, we can get the periodic support properties through LR PCs theory. From Fig. 2, we can find the pipe with LR structures can be transformed into the pipe with periodic support in the case of infinite oscillator mass m. Since the beginning frequency of the LR gap can be estimated as $1/2\pi\sqrt{k/m}$, the gap for the periodic support will start at 0 Hz for an infinite mass m. In the calculation, we suppose the density of the copper ring is $\rho_{Cu} = 8.95 \times 10^{10}\,\mathrm{kg\,m^{-3}}$. The complex band structure for the pipe with periodic support is illustrated in Fig. 12. The band gap frequency range is 0–49 Hz. The calculation results are the same as those in Ref. [13]

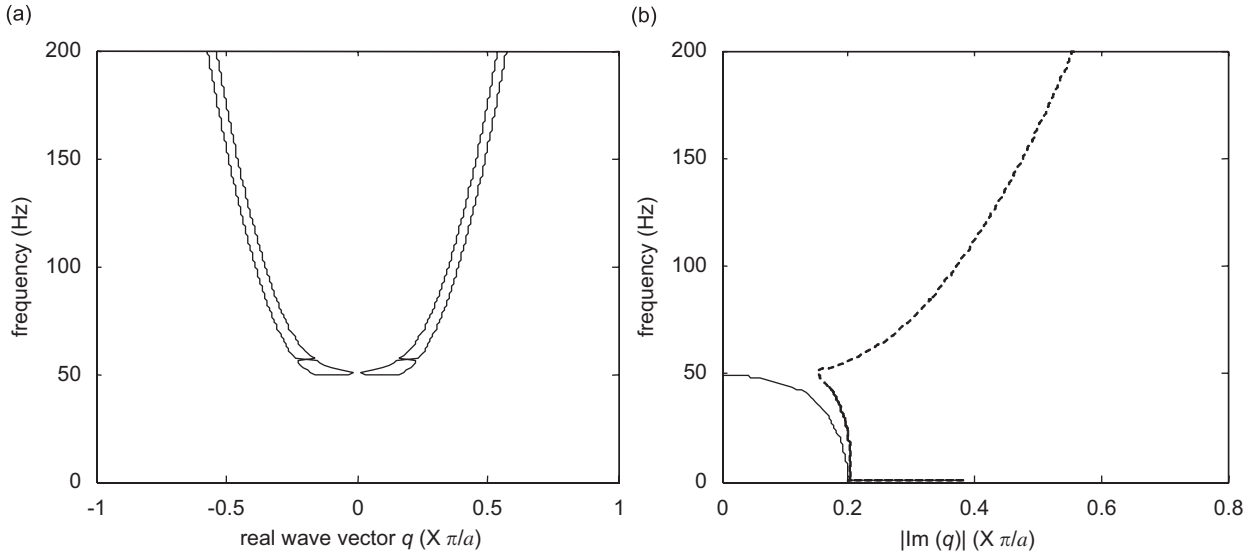

Fig. 12. Complex band structure of the pipe with fluid loading with infinite periodic support, the lattice constant $a = 0.75$ m.

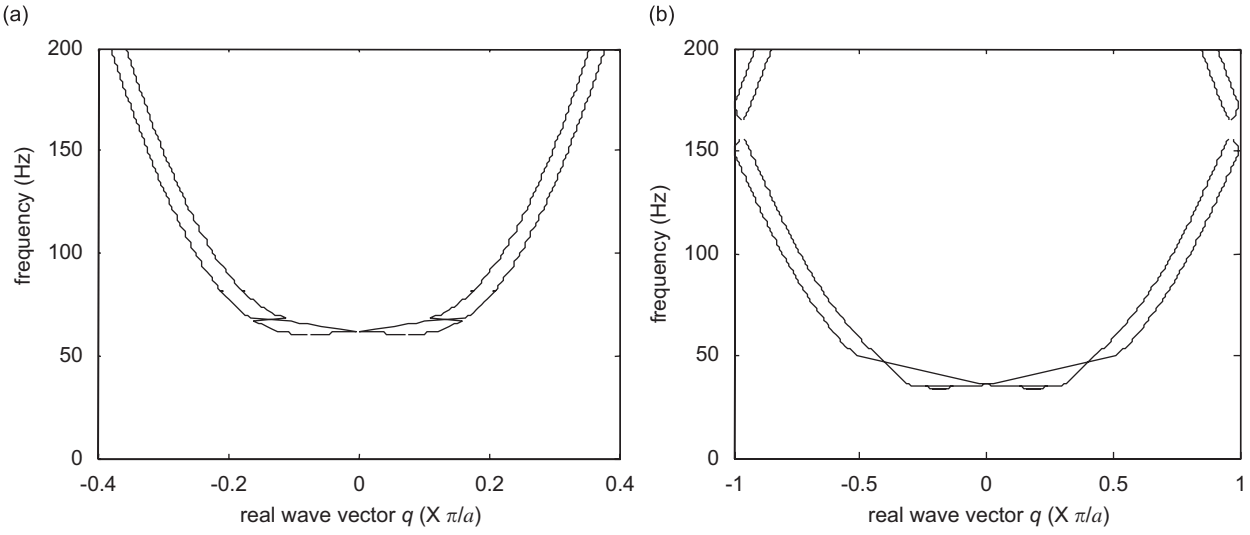

Fig. 13. Band structure of the pipe with fluid loading with infinite periodic support: (a) the lattice constant $a = 0.5$ m and (b) the lattice constant $a = 1.5$ m.

except for the different geometric and material parameters. From Fig. 12(b), one can find the typical characteristic of the Fano-like interference phenomena has disappeared. The lattice constant will affect the band gap frequency range illustrated in Fig. 13. The band gap frequency rings are 0–60 and 0–34 Hz for lattice constants $a = 0.5$ and 1.5 m, respectively.

4. Conclusions

In conclusion, the flexural vibration for a periodic pipe system with fluid loading is studied theoretically in this paper. Using the TM theory, the gap properties with Bragg scattering and LR mechanisms are studied.

For the Bragg scattering mechanism, the effect of the fluid load makes the gap frequency lower. Also, we find the gap frequencies are dependent on the internal fluid velocity. The gap frequencies become higher with faster velocity v.

For the LR mechanism, one can obtain the low-frequency gap with a small lattice constant. The effect of the fluid load will not change the beginning frequency of the LR gap.

By changing the lattice constant, the Bragg gap can couple with the LR gap. The benefit of the coupling between the Bragg scattering mechanism and LR mechanism is to widen the gap.

Finally, the pipe with LR structures can be transformed into the pipe with periodic support by changing some material parameters.

The existence of flexural vibration gaps in periodic pipe with fluid loading gives a new idea in vibration control of pipe. The findings will be significant in the application of band gaps.

Acknowledgements

This work was funded by the National Natural Science Foundation of China (Grant no. 50575222).

References

[1] D.J. Mead, Free wave propagation in periodically supported infinite beams, *Journal of Sound and Vibration* 11 (1970) 181–197.
[2] D.J. Mead, A new method of analyzing wave propagation in periodic structures: applications to periodic Timoshenko beams and stiffened plates, *Journal of Sound and Vibration* 104 (1986) 9–27.
[3] D.J. Mead, S. Markus, Coupled flexural–longitudinal wave motion in a periodic beam, *Journal of Sound and Vibration* 90 (1983) 1–24.
[4] M.S. Kushwaha, P. Halevi, L. Dobrzynski, et al., Acoustic band structure of periodic elastic composites, *Physical Review Letters* 71 (1993) 2022–2025.
[5] M.S. Kushwaha, P. Halevi, G. Martinez, L. Dobrzynski, B. Djafari-Rouhani, Theory of acoustic band structure of periodic elastic composites, *Physical Review B* 49 (1994) 2313–2322.
[6] M.M. Sigalas, E.N. Economou, Elastic and acoustic wave band structure, *Journal of Sound and Vibration* 158 (1992) 377–382.
[7] Z. Liu, X. Zhang, Y. Mao, Y.Y. Zhu, Z. Yang, C.T. Chan, P. Sheng, Locally resonant sonic materials, *Science* 289 (2000) 1734–1736.
[8] C. Goffaux, J. Sánchez-Dehesa, A. Levy Yeyati, P. Lambin, A. Khelif, J.O. Vasseur, B. Djafari-Rouhani, Evidence of Fano-like interference phenomena in locally resonant materials, *Physical Review Letters* 88 (2002) 225502.
[9] M. Hirsekorn, P.P. Delsanto, N.K. Batra, P. Matic, Modelling and simulation of acoustic wave propagation in locally resonant sonic materials, *Ultrasonics* 42 (2004) 231–235.
[10] Z. Liu, C.T. Chan, P. Sheng, Three-component elastic wave band-gap material, *Physical Review B* 65 (2002) 165116.
[11] J.H. Wen, G. Wang, D.L. Yu, et al., Theoretical and experimental investigation of flexural wave propagation in straight beams with periodic structures: application to a vibration isolation structure, *Journal of Applied Physics* 97 (2005) 114907.
[12] D.L. Yu, Y.Z. Liu, J. Qiu, G. Wang, H.G. Zhao, Complete flexural vibration band gaps in membrane-like lattice structures, *Physics Letters A* 357 (2006) 154–158.
[13] D.L. Yu, Y.Z. Liu, H.G. Zhao, G. Wang, J. Qiu, Flexural vibration band gaps in Euler–Bernoulli beams with two-degree-of-freedom locally resonant structures, *Physical Review B* 73 (2006) 064301.
[14] G.H. Koo, Y.S. Park, Vibration analysis of a 3-dimensional piping system conveying fluid by wave approach, *International Journal of Pressure Vessels and Piping* 67 (1996) 249–256.
[15] G.H. Koo, Y.S. Park, Vibration reduction by using periodic supports in a piping system, *Journal of Sound and Vibration* 210 (1998) 53–68.
[16] M.G. Kang, The influence of rotary inertia of concentrated masses on the natural vibrations of fluid-conveying pipes, *Journal of Sound and Vibration* 238 (2000) 179–187.
[17] S.Y. Lee, C.D. Mote Jr., A generalized treatment of the energetic of translating continua, part II: beams and fluid conveying pipes, *Journal of Sound and Vibration* 204 (1997) 735–753.

[18] C. Kittle, *Introduction to Solid State Physics*, Wiley, New York, 1986.
[19] H. Qiao, Q.S. Li, G.Q. Li, Vibratory characteristics of flexural non-uniform Euler–Bernoulli beams carrying an arbitrary number of spring-mass systems, *International Journal of Mechanical Sciences* 44 (2002) 725–743.
[20] D.L. Yu, Y.Z. Liu, G. Wang, H.G. Zhao, J. Qiu, Flexural vibration band gaps in Timoshenko beams with locally resonant structures, *Journal of Applied Physics* 100 (2006) 124901.
[21] A. Nougaoui, B. Djafari-Rouhani, Complex band structure of acoustic waves in superlattices, *Surface Science* 199 (1988) 623–637.
[22] G. Wang, X. Wen, J. Wen, L. Shao, Y. Liu, Two dimensional locally resonant phononic crystals with binary structures, *Physical Review Letters* 93 (2004) 154302.